Article

Not peer-reviewed version

Human Serum Enriched After Absorption of Fish Cartilage Hydrolysate Enhances the Healing of Primary Human Dermal Fibroblasts Through the Expression of Proteins with Anti-Inflammatory and Immunomodulatory Properties

Julie Le Faouder *, Aurelie Gueho, Regis Lavigne, Fabien Wauquier, Line Boutin-Wittrant, Elodie Bouvret, Emmanuelle Com, Yohann Wittrant, Charles Pineau

Posted Date: 8 December 2023

doi: 10.20944/preprints202312.0550.v1

Keywords: skin health; nutraceuticals; marine hydrolyzed collagen; marine collagen peptides; chondroitin sulfate; glycosaminoglycans; proteomics; wound healing; primary cells; human dermal fibroblasts; clinical; ex vivo

Article

Human Serum Enriched After Absorption of Fish Cartilage Hydrolysate Enhances the Healing of Primary Human Dermal Fibroblasts Through the Expression of Proteins with Anti-Inflammatory and Immunomodulatory Properties

Julie Le Faouder [1,2,*], Aurélie Guého [2], Régis Lavigne [2,3], Fabien Wauquier [4], Line Boutin-Wittrant [4], Elodie Bouvret [1], Emmanuelle Com [2,3], Yohann Wittrant [4,5,6,†] and Charles Pineau [2,3,†]

1 Abyss Ingredients, 860 route de Caudan, 56850 Caudan – France
2 Univ Rennes, CNRS, Inserm, Biosit UAR 3480 US_S 018, Protim Core Facility, F-35000 Rennes, France
3 Univ Rennes, Inserm, EHESP, Irset (Institut de Recherche en Santé, Environnement et Travail) – UMR_S 1085, F-35042 Rennes, France
4 Clinic'n'Cell SAS, 28 place Henri Dunant, 63000 Clermont-Ferrand, France
5 INRAE, UNH, 63009 Clermont-Ferrand, France
6 Clermont Auvergne University, 63000 Clermont-Ferrand, France
* Correspondence: julie@abyss-ingredients.com; Tel.: +33-(0)601827451
† These authors contributed equally to this work.

Abstract: Our skin epidermis constitutes the most important innate defense barrier against all pathogens. Therefore, even if skin lesions are common due to infections, scarring, genetic disorders, and other diseases, skin integrity is crucial for maintaining body homeostasis. Marine collagen peptides (MCPs) and Glycosaminoglycans (GAGs) have been described as potential wound healing (WH) agents. Recently, through an ex vivo clinical approach, we have demonstrated the nutricosmetic potential of fish cartilage hydrolysate (FCH), which presents a combination of collagen peptides and GAGs. Here, we coupled a clinical approach with in vitro experiments on human dermal fibroblasts (HDFs) and applied a Data Independent Acquisition - Parallel Accumulation Serial Fragmentation (diaPASEF) proteomic analysis, to assess the potential benefit of FCH in WH and its mode of action. Our results show that human serum enriched with circulating metabolites resulting from FCH ingestion, improved wound closure in scratch assays. In support, some proteins with anti-inflammatory and immunomodulatory properties or prone to promote hydration and extracellular matrix (ECM) stability showed increased expression in HDFs, after exposure to FCH-enriched serum. These findings suggest that FCH appears as a promising nutrient for WH and skin regeneration.

Keywords: skin health; nutraceuticals; marine hydrolyzed collagen; marine collagen peptides; chondroitin sulfate; glycosaminoglycans; proteomics; wound healing; primary cells; human dermal fibroblasts; clinical; ex vivo

1. Introduction

Our skin epidermis constitutes the most important innate defense barrier against all pathogens and plays an important role in tissue homeostasis [1]. Skin lesions may originate from common interactions with its environment (burns, infections, scarring, dryness…), genetic disorders, and other diseases [2,3]. Atopic dermatitis (AD) is a major chronic inflammatory skin disease caused by a complex interplay between the immune system, skin barrier abnormalities and deregulation of cutaneous microbiome [4,5]. Beside AD, psoriasis prevalence is high. Psoriasis alters skin, nails, and

 doi:10.20944/preprints202312.0550.v1

joints. It is caused by multigenic predisposition, environmental factors, and aberrant immune response [6]. Restoring skin integrity involves multidimensional processes such as inflammation, proliferation, epithelialization, angiogenesis, remodeling, and healing [7].

Marine collagen peptides (MCPs) have been shown to be an effective biomaterial for wound healing (WH) and skin regeneration [8]. They are produced from collagen through both chemical and enzymatic hydrolysis. Their low molecular weight increases their water solubility, making them more assimilable and absorbable [9]. Hu et al. demonstrated that MCPs isolated from the skin of tilapia improved wound closure in an in vitro scratch assay, with the concentration of 50.0 $\mu g.mL^{-1}$. They also demonstrated that the application of MCPs could enhance the process of WH in experiments of deep partial-thickness scald wound in rabbits. [10]. Several groups have shown beneficial effects of MCP supplementation on skin healing in rats. Yang et al. demonstrated that oral administration of MCPs isolated from Alaska pollock, to wounded rats, significantly increased recovery rates and hydroxyproline content compared to the control groups. The treated group showed a near-normal epidermis structure on day 12 of healing, while control group displayed poor re-epithelialization [11]. Wang et al. found that oral administration of MCPs prepared from salmon skin, improved WH following cesarean section in rats. The treated group showed increased level of hydroxyproline and elevated fibroblast proliferation and vascularization at 7 days post-treatment, compared to control group [12]. Similarly, Zhang et al., demonstrated that oral administration of MCPs from chum salmon skin enhanced cutaneous WH and angiogenesis in rats. Improved vascularization, epithelization, and fibroblast infiltration were observed in the treated groups, as well as elevated levels of hydroxyproline [13].

Glycosaminoglycans (GAGs) from marine sources, essential components of the bone and cartilage tissues, have been described as potential therapeutic agents, and particularly as anti-inflammatory agents. They are all linear polysaccharide chains composed of repeating disaccharide units, which can be differently sulphated, generally grouped into four groups: hyaluronic acid (HA) or hyaluronan; keratan sulfate; heparan sulfate/heparin; and chondroitin sulfate (CS)/dermatan sulfate (DS) [14]. CS/DS chains isolated from fish cartilage were shown to have significant anti-inflammatory activity. In vitro, Campo et al. demonstrated that CS from shark cartilage reduced inflammation mediators and apoptosis in mouse articular chondrocytes after stimulation with lipopolysaccharides (LPS) [15]. More recently, addition of CS from shark cartilage to mouse bone-marrow derived macrophages stimulated with LPS and interferon-γ, produced a reduction in both, NO and pro-inflammatory cytokines release and an increase of the anti-inflammatory cytokine interleukin-10 [16]. A similar trend was observed for fish cartilage hydrolysate (FCH) in primary human articular chondrocytes [17]. Marine GAGs were also shown to impact wound repair. Krichen et al. showed that the application of GAGs from fish skins-based gels, on dermal full-thickness excision wounds in a mouse model, enhanced significantly WH activity. The treatment reduced the edema after carrageenan injection, protected edema tissue from oxidative damage and reduced the risk of inflammation [18].

Recently, through an ex vivo clinical approach, we have demonstrated the nutricosmetic potential of FCH, which presents a combination of collagen peptides and GAGs. Indeed, the human serum enriched with circulating metabolites resulting from FCH ingestion (FCH-enriched serum), stimulated the growth of human dermal fibroblasts (HDFs), promoted the specific production of hyaluronan, up-regulated the synthesis of elastin and inhibited the expressions of matrix metalloproteinases (MMP)-1 and 3 along with an increase in TGF-β release. Thus, FCH promotes hydration, elasticity and limits the expression of catabolic factors involved in photoaging [19]. Additionally, it was previously showed that supplementation of middle-aged healthy women with this FCH led to both, a significant reduction in wrinkles and an increase of dermis density [20]. Here, we continued to investigate the potential benefit of FCH in human skin functionality. By coupling our *ex vivo* clinical approach with a Data Independent Acquisition - Parallel Accumulation Serial Fragmentation (diaPASEF) proteomic analysis, we explored the effects of FCH-enriched serum in WH and its potential mode of action.

Preprints (www.preprints.org) | NOT PEER-REVIEWED | Posted: 8 December 2023 doi:10.20944/preprints202312.0550.v1

2. Results

2.1. FCH-Enriched Serum Improved HDF Migration during Wound Healing Assay

As previously described [19], according to the circulating hydroxyproline and CS concentration profiles, the collection of human FCH-enriched serum was set at 140 min post-ingestion. Moreover, we previously showed that human serum, enriched or not, had no cytotoxic effect on HDFs cultures.

To investigate the potential benefit of FCH in skin healing, primary HDFs were subjected to migration assays in order to evaluate their capacity to cover a wounded surface. As shown in Figure 1A, the wounded area was rapidly colonized by migrating fibroblasts in the presence of human serum. A higher colonization was observed in the presence of human FCH-enriched serum. This improved migration was significant at 6 h: 9.5% H-NAIVE serum vs 15.5% H-FCH serum covered surface; in others words, the increase reaches +64% of covered surface and tended to be significant at 12 h (p=0.06; 34.2% vs 41.8%) (Figure 1B).

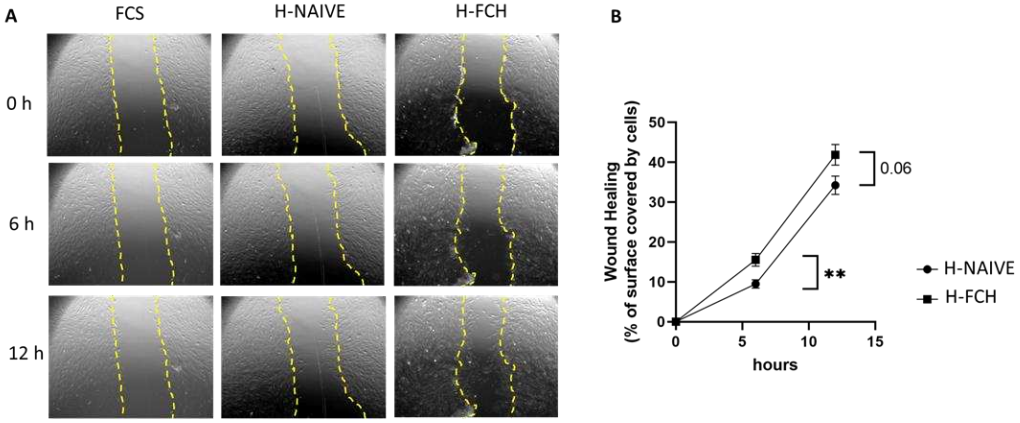

Figure 1. Evolution of HDF migration during wound healing assay. (**A**): Representative view at 0, 6 and 12h. (**B**): Percentage of covered surface by cell over time.

2.2. FCH-Enriched Serum Modulates Protein Expression Involved in Healing

Primary HDFs were subjected to proteomic study in order to evaluate the underlying mechanisms of FCH on skin functionality. In the overall series (n = 20), 6,842 proteins were quantified from HDFs (Supplementary Table S1). PCA of the quantified proteins discriminated H-NAIVE group from H-FCH one (Figure 2), supporting that the expression of HDF proteins was modulated by FCH-enriched serum.

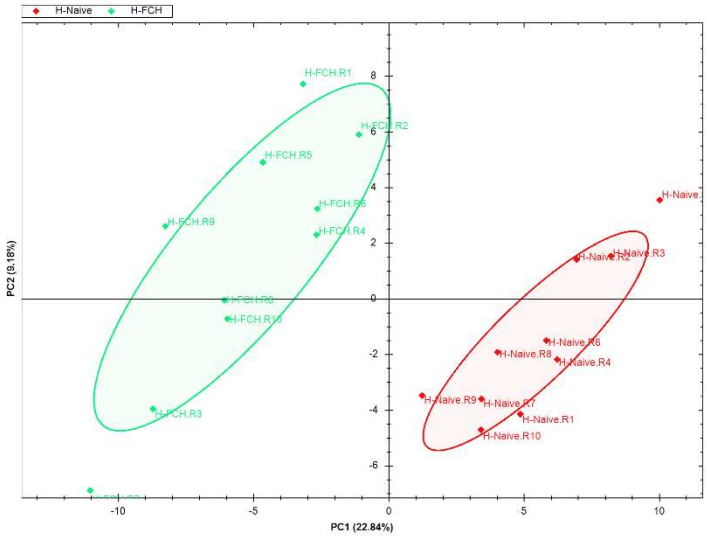

Figure 2. Evaluation of quantified HDF proteins. Graphic representation defined by the first two principal components (PC1 and 2) of the principal component analysis (PCA).

 doi:10.20944/preprints202312.0550.v1

T-test displayed 195 differential proteins (Q < 0.05; absolute log2 ratio of 0.58) between H-FCH and H-Naive, with 122 and 73 proteins over- and under expressed in H-FCH, respectively (Supplementary Table S2).

Clustering of the 195 differential proteins revealed six clusters (C1-C6) (Figure 3A, Supplementary Table S3). Two clusters brought together proteins with increased expression following the exposition to FCH-enriched serum (C1, C2). Proteins upregulated in cluster C1 and C2 corresponded to enrichment in pathways such as acute inflammatory response (cluster frequency 19/91 (20.8%), corrected $p = 1.0068.10^{-17}$), immune response (cluster frequency 27/91 (29.6%), corrected $p = 1.8098.10^{-16}$), response to wounding (cluster frequency 23/91 (25.2%), corrected $p = 1.1189.10^{-11}$), and glycosaminoglycan binding (cluster frequency 5/91 (5.4%), corrected $p = 1.8467.10^{-2}$) (Figure 3B, Supplementary Table 3). Some of these pathways and the associated proteins are presented in Table 1. All proteins in the acute inflammatory response GO term are common to response to wounding one. Likewise, from the 27 proteins in the immune response GO term, 10 are common to response to wounding one.

Preprints (www.preprints.org) | NOT PEER-REVIEWED | Posted: 8 December 2023 doi:10.20944/preprints202312.0550.v1

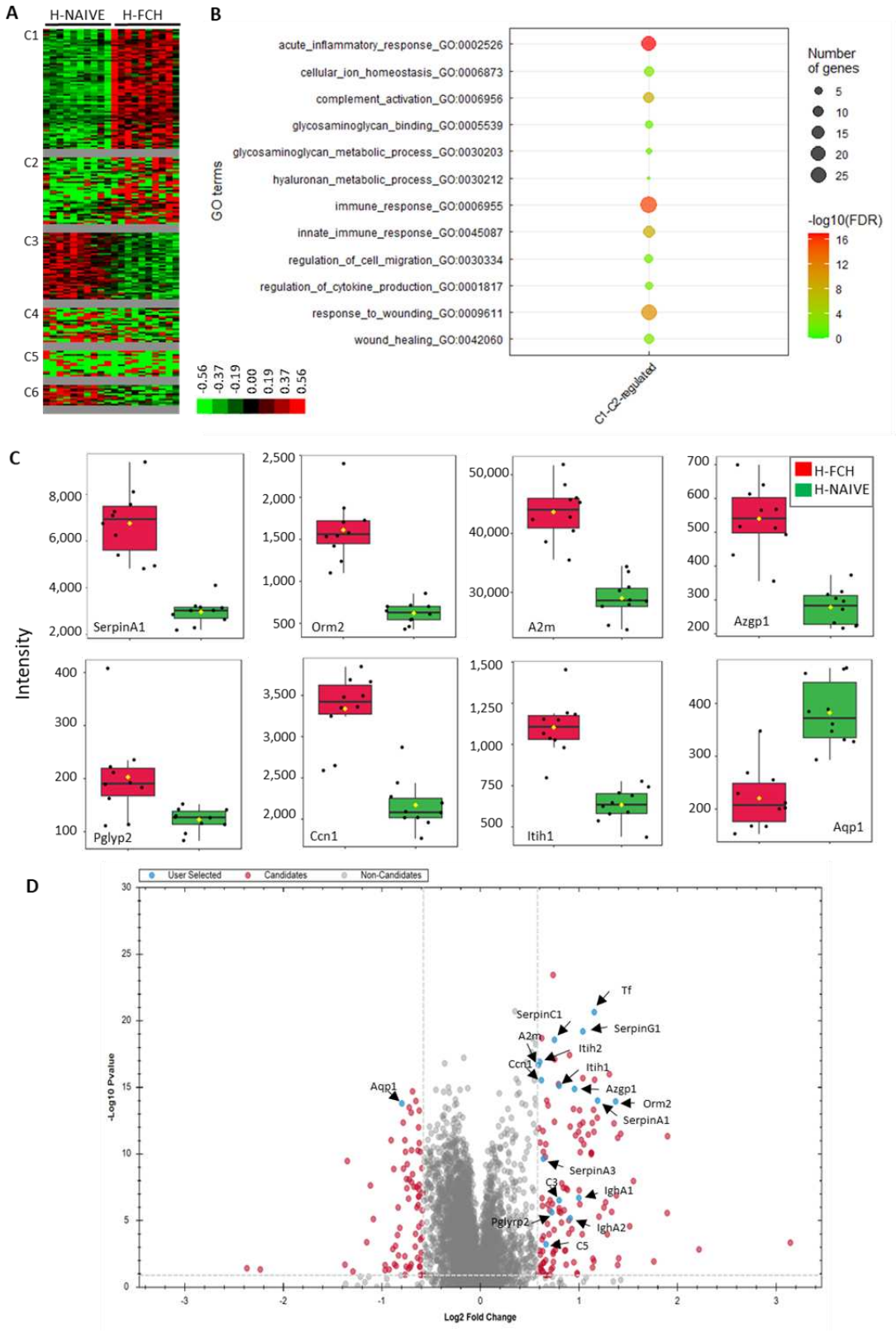

Figure 3. Proteins differentially expressed between H-NAIVE and H-FCH (n = 195). (**A**): Unsupervised Bayesian clustering (n = 10/group). (**B**): Gene ontology (GO) term enrichment for proteins upregulated by FCH-enriched serum from cluster C1-C2. (**C**): Boxplots representing normalized abundances of differentially expressed proteins. (**D**): Volcano plot representing the statistical comparison of the protein intensities of H-FCH versus H-NAIVE. The abscissa reports the fold change in logarithmic scale (difference), and the ordinate −log(Q) of t-tests. Some deregulated proteins involved in healing have been annotated and highlighted in blue.

Preprints (www.preprints.org) | NOT PEER-REVIEWED | Posted: 8 December 2023 doi:10.20944/preprints202312.0550.v1

Table 1. Pathways and their associated proteins upregulated by FCH-enriched serum.

Pathway	Protein IDs	Gene name	Protein name
Response to wounding	P01023	A2M	Alpha-2-macroglobulin
	P02743	APCS	Serum amyloid P-component
	P02652	APOA2	Apolipoprotein A-II
	P02749	APOH	Beta-2-glycoprotein 1
	P02746	C1QB	Complement C1q subcomponent subunit B
	P02747	C1QC	Complement C1q subcomponent subunit C
	P09871	C1S	Complement C1s subcomponent
	P06681	C2	Complement C2
	P01024	C3	Complement C3
	P01031	C5	Complement C5
	P02748	C9	Complement component C9
	P21926	CD9	CD9 antigen
	P00751	CFB	Complement factor B
	P08603	CFH	Complement factor H
	P00742	F10	Coagulation factor X
	P02763	ORM1	Alpha-1-acid glycoprotein 1
	P19652	ORM2	Alpha-1-acid glycoprotein 2
	P35542	SAA4	Serum amyloid A-4 protein
	P01009	SERPINA1	Alpha-1-antitrypsin
	P01011	SERPINA3	Alpha-1-antichymotrypsin
	P01008	SERPINC1	Antithrombin-III
	P05155	SERPING1	Plasma protease C1 inhibitor
	P02787	TF	Serotransferrin
Immune response	P25311	AZGP1	Zinc-alpha-2-glycoprotein
	P02746	C1QB	Complement C1q subcomponent subunit B
	P02747	C1QC	Complement C1q subcomponent subunit C
	P09871	C1S	Complement C1s subcomponent
	P06681	C2	Complement C2
	P01024	C3	Complement C3
	P01031	C5	Complement C5
	P02748	C9	Complement component C9
	P00751	CFB	Complement factor B
	P08603	CFH	Complement factor H
	Q92989	CLP1	Polyribonucleotide 5'-hydroxyl-kinase Clp1
	P32456	GBP2	Guanylate-binding protein 2
	P01876	IGHA1	Immunoglobulin heavy constant alpha 1
	P01877	IGHA2	Immunoglobulin heavy constant alpha 2
	P01857	IGHG1	Immunoglobulin heavy constant gamma 1
	P01859	IGHG2	Immunoglobulin heavy constant gamma 2
	P01860	IGHG3	Immunoglobulin heavy constant gamma 3
	P01861	IGHG4	Immunoglobulin heavy constant gamma 4
	P01871	IGHM	Immunoglobulin heavy constant mu
	P01834	IGKC	Immunoglobulin kappa constant
	P01602	IGKV1-5	Immunoglobulin kappa variable 1-5
	P04433	IGKV3D-11	Immunoglobulin kappa variable 3-11
	A0A0C4DH25	IGKV3D-20	Immunoglobulin kappa variable 3D-20
	P06312	IGKV4-1	Immunoglobulin kappa variable 4-1
	Q96PD5	PGLYRP2	N-acetylmuramoyl-L-alanine amidase

 doi:10.20944/preprints202312.0550.v1

	Q9Y535	POLR3H	DNA-directed RNA polymerase III subunit RPC8
	P05155	SERPING1	Plasma protease C1 inhibitor
Glycosaminoglycan binding	Q96PD5	PGLYRP2	N-acetylmuramoyl-L-alanine amidase
	P01008	SERPINC1	Antithrombin-III
	P02749	APOH	Beta-2-glycoprotein 1
	O00622	CCN1	CCN family member 1
	P47914	RPL29	60S ribosomal protein L29
Glycosaminoglycan metabolic process	Q96PD5	PGLYRP2	N-acetylmuramoyl-L-alanine amidase
	P19823	ITIH2	Inter-alpha-trypsin inhibitor heavy chain H2
	P19827	ITIH1	Inter-alpha-trypsin inhibitor heavy chain H1

Two clusters brought together proteins with decreased expression following the exposition to FCH-enriched serum (C3 and C6) (Supplementary Table S3). Proteins from these clusters did not display pathway enrichment but matched with the terms: metabolic process (cluster frequency 28/40; with protein such as 9S ribosomal protein L23, mitochondrial (L23mt), MRP-L23), catalytic activity (cluster frequency 20/40; e.g., Alpha-1,2-mannosyltransferase, ALG9), and organelle part (cluster frequency 20/40; e.g., Aquaporin-1, AQP-1).

Some of the differential proteins further described in the discussion are illustrated in Figures 3C and D, representing their normalized intensity and their statistical comparison between H-NAIVE and H-FCH.

3. Discussion

In this study, to investigate the potential benefit of FCH in human skin functionality, we first set an ex vivo experiment combining the clinical digestive course of nutrients with in vitro assays. This approach represents a physiologic and ethic alternative to preclinical studies giving in vitro models a clinical dimension to evaluate the impact of the metabolized compounds in a nutraceutical context [21–25]. Then, we performed a diaPASEF proteomic analysis, allowing the detection of proteome in depth [26,27], to explore the mechanism of action of human FCH-enriched serum on HDFs.

Our precedent study demonstrated the beneficial effects of FCH for nutricosmetic applications, by supporting hydration, elasticity and limiting the expression of catabolic factors involved in photoaging [19]. Here, we studied whether FCH could promote the healing process, using a mimicking fibroblast lesion in vitro. FCH-enriched serum led to an increase in cell confluence in the wounded area after scratch wound assays performed on HDFs. This increase was consistent with the enhancement of the viability and proliferation by FCH-enriched serum, previously observed in XTT tests after 48h incubation [19]. Therefore, FCH may enhance proliferation and migration of HDFs. However, here, enhanced migration was observed from 6 hours incubation thus supporting a specific enhancement of cell migration process rather than a simple proliferation artefact. To date, there was no impact of FCH-enriched serum on HDF proliferation after 24h incubation. As mentioned above, MCPs and marine GAGs, to a lesser extent, are studied for their facilitating role in the healing process [8,10–13,18]. Indeed, they may support skin tissue engineering by promoting both the proliferation and migration of primary HDFs and the differentiation and the migration of human keratinocytes as well [8,28]. Besides, we previously observed that FCH-enriched serum increased the release of TGF-β [19], which is also involved in fibroblast proliferation and keratinocyte differentiation in WH [29,30]. Taken together, these results indicate that FCH appears as a promising nutrient for WH and skin regeneration.

Thanks to our proteomic strategy, we consistently show that FCH-enriched serum upregulated proteins relative to response to wounding, and in particular several members of the serpin family. Serpins (serine protease inhibitors or classified inhibitor family I_4) are a broadly distributed family of protease inhibitors that use a conformational change to inhibit target enzymes. They are central in controlling many important proteolytic cascades, including the mammalian coagulation pathways [31]. Serpins are of particular interest in WH due to their inhibitory effects on specific proteases that are relevant to wound response including inflammation, ECM remodelling, cell migration and proliferation [32]. Alpha1-antitrypsin (SERPINA1), has been described to reduce the activity of MMP-

 doi:10.20944/preprints202312.0550.v1

9, as well as the anti-inflammatory and the anti-apoptotic effects during the healing response [33,34]. Likewise, serpin A1, known as a potent inhibitor of neutrophil elastase, which hydrolyzes proteins including elastin, has therapeutic potential as a wound-healing agent [35]. Furthermore, alpha1-antichymotrypsin (SERPINA3) displayed similar effects to alpha1-antitrypsin during the healing by accelerating wound closure in an experimental dermal open wounds in rabbits [36]. Finally, it was shown that local administration of plasma protease C1 inhibitor (SERPING1) provided inhibition of edema formation, reduction of inflammatory tissue damage and increased re-epithelialization in experimental cutaneous burn lesions in animals [37,38]. We previously demonstrated that FCH-enriched serum inhibited MMP-1 and 3 expression while increasing elastin production in HDFs [19]. Here, we have confirmed this increase using a proteomic approach (elastin: q value = $1.94.10^{-6}$; absolute log2 ratio = 0.52) (Supplementary Table S2).

FCH-enriched serum also induced the upregulation of several members of the complement activation pathway. Best known for its role in immune surveillance and inflammation, there is increasing evidence that complement activation contributes to tissue repair [39]. Thus, increased collagen/fibronectin levels and enhanced WH were seen after topical application of complement C3 and -5 to rat skin wounds [40,41]. Other proteins from the response to wounding pathway, such as serotransferrin (TF), alpha-2-macroglobulin (A2M) or alpha1-acid glycoprotein (ORM) 1 and -2 were also upregulated by FCH-enriched serum. Indeed, TF was considered a potential wound-healing mediator in human nasal fibroblast conditioned medium [42]. The different effects (*e.g.,* stimulation of cell proliferation and migration, interaction with collagen) of A2M and ORM, proteins with anti-inflammatory and immunomodulating properties, may suggest a beneficial role in WH [43,44].

As aforementioned for several members of the complement activation pathway, FCH-enriched serum upregulated proteins involved in the immune response. This also includes immunoglobulins. Indeed, constant region heavy chains of immunoglobulin A (1,2), G (1-4) and M, as well as constant and variable domain of immunoglobulin light chains, were increased. Nishio and collaborators demonstrated that B cells, which produce antibodies to damaged tissues, were engaged in the process of WH. Indeed, they showed that splenectomy delayed WH, and that the transfer of spleen cells into splenectomized mice recovered the delay in WH. Additionally, these authors showed that immunoglobulin G1 (IgG1) bound to wounded tissues and that splenectomy reduced the amount of IgG1 binding to wounded tissues [45].

Additionally, FCH-enriched serum induced the upregulation of other proteins involved in the immune response, that have been described for their beneficial roles in skin pathologies such as AD and psoriasis (*e.g.,* zinc-alpha-2-glycoprotein (AZGP1, ZAG), guanylate-binding protein 2 (GBP2) and N-acetylmuramoyl-L-alanine amidase (PGLYRP2)). Noh *et al.* reported a role for zinc-alpha-2-glycoprotein in AD pathogenesis and demonstrated that topical treatment with this protein, restored skin barrier integrity and limited AD inflammation [46]. The guanylate-binding protein 2 is part of the GBP family, which is mainly known for its diverse activity against invading microbes and pathogens, as a part of innate immune response [47]. Bowcock et al. found GBP1 and 2 transcripts differentially expressed in involved psoriatic skin versus normal skin [48]. Peptidoglycan Recognition Proteins (PGRPs or Pglyrps) represent a class of innate immunity proteins expressed in the skin. Park *et al.* demonstrated that Pglyrp2 protected mice from psoriasis-like skin inflammation by promoting Treg and limiting Th17 responses [49]. Overall, these results confirm the healing promotion properties of FCH-enriched serum and suggest the induction of potential anti-inflammatory and immunomodulatory properties that should be further investigated in skin pathologies.

Finally, FCH-enriched serum upregulated proteins related to GAG binding such as CCN family member 1 (CCN1), an heparin-binding, extracellular matrix-associated protein which appears to play a role in WH by up-regulating the expression of a number of genes involved in angiogenesis, inflammation and matrix remodeling (e.g., MMP1 and MMP3) in skin fibroblasts [50]. FCH-enriched serum also induced the upregulation of polypeptides involved in GAG metabolic process such as inter-alpha-trypsin inhibitor heavy chain H1 and -2 (ITIH1, ITIH2). Recent in vivo and in vitro studies have shown that HC1 and HC2 are linked to HA resulting in the improvement of ECM stability [51].

 doi:10.20944/preprints202312.0550.v1

To note, we previously highlighted that HA synthesis was significantly stimulated in the presence of FCH-enriched serum [19]. Aquaporin-1 (AQP-1), one of the down-regulated proteins by FCH-enriched serum, is a water channel protein controlling the water contents of cells and tissues. It exerts pleiotropic effects on various biological activities, including inflammation, angiogenesis, and ECM remodeling, by regulating cell behaviors and tissue water balance. AQP1 was shown to be up-regulated in systemic sclerosis dermal fibroblasts and endothelial cells, possibly contributing to inflammation, vasculopathy, and tissue fibrosis by regulating tissue edema and cell migration [52]. Thus, FCH could contribute to skin functionality by promoting hydration and ECM stability.

Our study had several limitations. We investigated HDF proteome, comparing the influence of human FCH-enriched serum *versus* naive human serum. First of all, despite all skills used to carefully wash the cells and remove supernatant prior to proteomic investigation on HDFs, we cannot exclude that some of the differential observed proteins originate from the serum. Indeed, immunoglobulins are produced by B cells rather than HDFs, therefore, the observed difference in this class of protein more likely result from immunoglobulins attached to HDFs. In this light, one may also question the difference regarding the proteins of the complement complex. In this case, fibroblasts from the dental pulp have been reported to express all the proteins required for efficient complement activation, including C5b-9 and C5a [53]. More specifically, at the skin level, HDFs were previously demonstrated to successfully produce complement protein C4 [54], C1r and C1s [55]. Thus, even if a bias may occur for certain class of proteins, a differential expression still remains between the two conditions and clearly indicates a potent and positive impact of FCH on HDFs metabolism. On another hand, we performed the proteomic analysis in the absence of scratching, to avoid bias due to fibroblast lesion. It would have been also relevant to study HDF proteome upon scratching or in a context of IL-1β-induced inflammation, in order to get a global overview of the influence of FCH-enriched serum during WH or inflammation processes. HDF are key cellular players in regulating skin health, however, additional investigations on human primary keratinocytes may further provide clues on the possible influence of FCH-enriched serum on the keratinocytes/fibroblast cross-talks and their positive impact on skin health. Similarly, more complex and physiologically relevant models that involve the co-culture of primary keratinocytes and fibroblasts [56], or skin organoids encompassing the epidermis, dermis, and appendages [57], could be considered. Ideally, we would like to explore the effect of FCH-enriched serum on human skin explants to best fit structural and physiological resemblance to live skin tissue. They contain all resident cell populations from tissue, conserve their barrier function as well as the differentiation of the epidermal layer and the ECM composition. Above all, they can be healthy or lesional [58]. Thus, we could evaluate the potential beneficial effects of FCH on skin explant models of DA or psoriasis Finally, it would be of great interest to study the effects of FCH-enriched serum on the skin microbiome.

4. Materials and Methods

4.1. Experimental Design

4.1.1. Ethics and Clinical Trial

The clinical part of the protocol was approved by the French Ethical Committee (2021-ND77 RIPH2 HPS/N° SI RIPH: 21.01436.000014/N° EudraCT/ID RCB: 2021-A01773-38/Comité de Protection des Personnes CPP Paris, Ile-de-France 1; approved 08 October 2021). The investigation was conducted with respect regarding the Declaration of Helsinki of 1975 (https://www.wma.net/what-we-do/medical-ethics/declaration-of-helsinki (accessed on)) revised in 2013. All volunteers were informed about the objectives and the potential risks of the investigation. Their written informed consent was obtained before their recruitment.

4.1.2. Product Tested

Fish cartilage hydrolysate (FCH) is a water-soluble powder obtained from a standardized manufacturing process based on an enzymatic hydrolysis of marine fish cartilage, without

 doi:10.20944/preprints202312.0550.v1

preservatives or processing aids (Abyss Ingredients, Caudan, France). Its natural composition, containing 65% collagen peptides and 25% of chondroitin sulfate has been determined by Dumas and Scott assays, respectively. The molecular weight distribution of collagen peptides was determined by gel permeation HPLC-UV: more than 98% have a molecular weight under 3000 Da and 80% under 1000 Da (Figure S1). These analyses were carried out by accredited laboratories (COFRAC). FCH was given at the dose of 12 g per intake and per volunteer. A single dose corresponded to an acute exposure to 8.04 g of hydrolyzed collagen and 3.24 g of chondroitin sulfate.

4.1.3. Human Study Protocol

A pool of 10 healthy men (age: 25.4 years old, +/−3.7; BMI: 23.6 kg/m2, +/−1.9; >60 kg; without drug treatment; and no distinction on ethnicity) was recruited for this study. Before participation, all volunteers were checked for normal ranged blood formulation, renal (urea and creatinine) and liver functions (aspartate aminotransferase (AST), alanine aminotransferase (ALT), gamma-glutamyltransferase (GGT) activities) to ensure volunteer safety and accurate data collection. Blood samples were performed, teched, aliquoted and stored at the Centre d'Investigation Clinique de Clermont-Ferrand - Inserm U1405. The clinical part comprised two phases. The first one was dedicated to validate and determine the human FCH's metabolites absorption profile. Ten fasted volunteers received 12 g of FCH and were subjected to blood sampling. Nine mL of venous blood were collected before the ingestion and every 20 min for 240 min after the ingestion. Serum was separated from blood cells and immediately stored at −80 °C until further analyzed. The second phase was set to collect both naive and FCH-enriched serum fractions. As for the first step, 10 healthy volunteers fasted for 12 h and were then given 12 g of FCH. A total of 48 mL of venous blood was collected before the ingestion for naive (baseline) serum collection. Then, at the maximum absorption peak, 48 mL of blood as well was collected for metabolites-enriched serum collection. Serum was stored at −80 °C until analysis.

4.1.4. Human Primary Dermal Fibroblasts (HDFs) Cultures

HDFs were obtained from an adult donor (Sigma-Aldrich, Lyon, France, 106-05A). For maintenance, primary cells were cultured in Dulbecco's Modified Eagle Medium (DMEM, Biowest, L0066-500) supplemented with 10% fetal calf serum (FCS) (Invitrogen Corporation, Illkirch, France) and 1% penicillin/streptomycin (Life Technologies, Villebon-Sur-Yvette, France). Cells were cultured at 37 °C and 5% CO2/95% air.

4.2. Wound Healing

4.2.1. Cell Treatment

Cells were seeded at the density of 15,000 cells/cm^2 in 24-wells plates with 500 µL of culture medium and allowed to grow in maintenance media in order to reach 80% - 90% confluency. Cells were then incubated in DMEM supplemented with 1% penicillin/streptomycin in the presence of 10% of human naive serum (H-NAIVE) or human serum enriched with circulating metabolites resulting from FCH ingestion (H-FCH) according to the Clinic'n'Cell protocol. After 24 h of pre-treatment, monolayers of dermal fibroblasts were subjected to a linear scratch in the middle of the well using a P1000-tip. Then, culture media were changed to removed floating cells and scratched monolayers were placed under a videomicroscope allowing timelapse investigations at 37°C and 5%CO2/95%air. X, Y and Z coordinates were set for each well to follow the migration of the primary HDFs covering the scratched area on 24h. Human serum were not pooled and each monolayer was incubated with one particular serum (H-NAIVE, n=10; H-FCH, n=10). Surface covered by cells was quantified using ImageJ software 1.53 and calculated as a percentage (ratio) of the initial wounded surface to avoid bias in comparison.

 doi:10.20944/preprints202312.0550.v1

4.2.2. Statistics

Prism V.9.4.1 (GraphPad Software, San Diego, CA, USA) was used to run statistic tests and set figures. The following statistic plan was applied: Gaussian distribution was evaluated according to Shapiro–Wilk normality test. In case of non-normal distribution, a Kruskal–Wallis nonparametric test was used followed by Dunn test for *post hoc* comparison. When normal distribution and equal variance were assumed, measures were subjected to one-way ANOVA with Tukey's test for multiple comparisons. Values are presented as the means ± SD unless specified otherwise. The differences were considered statistically significant with * for $p < 0.05$, ** for $p < 0.01$, *** for $p < 0.001$ and **** for $p < 0.0001$.

4.3. DiaPASEF Proteomic Analysis

4.3.1. Cultures for diaPASEF Proteomic Analysis

Cells were seeded at the density of 15,000 cells/cm^2 in 12-wells plates with 1 mL of culture medium and grown for 3 days in maintenance media in order to reach 70% confluency. Cells were then incubated in DMEM supplemented with 1% penicillin/streptomycin in the presence of 10% of H-NAIVE or H-FCH serum according to the Clinic'n'Cell protocol. After 24 h of incubation either with the naive or the enriched human serum fraction, culture supernatants were discarded and cells were washed two times with ice-cold isotonic buffer (PBS). Remaining liquid was carefully removed from the well and the cell monolayer was immediately stored at -80°C. By the time the cells were frozen, cultures approximately reached 85% confluency for about 200 000 cells/well (per tested condition).

4.3.2. Sample Preparation for diaPASEF Analysis

Each cell samples were solubilized, reduced, alkylated, digested and desalted using the PreOmics IST kit (PreOmics GmbH, Martinsried, Germany). Briefly, each sample was resuspended in 70 µL of IST Lysis buffer, and reduced and alkylated for 10 min at 95°C under 1000 rpm shaking condition. After BCA assay, 10 µg of each sample were digested by addition of 50 µL of Digestion PreOmics Mix (Trypsin and LysC) and incubation at 37°C for 3 h. Digested samples were then desalted according to manufacturer's instructions and dried by vacuum centrifugation. Dried peptides were resuspended in PreOmics LC-LOAD buffer at a concentration of 100 ng/µL.

4.3.3. Sample Preparation for Spectral Library

For construction of a spectral library, a pool of 10 µg of proteins was prepared for each condition by pooling 1 µg of each protein sample. Pools were then separated onto an SDS-PAGE gel (Nu-PAGE 4-12 %, Invitrogen) for 45 min at 200 V, and the gel was further stained with ReadyBlue™ Protein Gel Stain (Sigma-Aldrich, St. Louis, MO, USA). Each lane was cut into 12 strips which were processed for in-gel digestion as previously described [59], using 4 ng.µL^{-1} of a Tryspine/LysC mix (v5073, Promega, Madison, WI, USA) in 25 mM ammonium bicarbonate / 0,01% ProteaseMAX™ (Promega). Each fraction was then desalted using the Phoenix kit (PreOmics).

4.3.4. Nanoliquid Chromatography Coupled with Tandem Mass Spectrometry (NanoLC-MS/MS) Acquisition of Fractions for Spectral Library–DDA-PASEF

All fractions (n = 12) of the different pools were analysed in Data-Dependent Analysis (DDA) and PASEF mode to generate the spectral library. Each fraction of enzymatically digested proteins (about 200 to 300 ng) was separated onto a 75 µm × 250 mm IonOpticks Aurora 3 C18 column (Ion Opticks Pty Ltd., Bundoora, Australia). A gradient of reversed phase buffer (Buffer A: 0.1% formic acid, 2% acetonitrile, 97.9% H2O; Buffer B: 0.1% formic acid, 99,9% acetonitrile) was run on a nanoElute UHPLC System (Bruker Daltonik GmbH, Bremen, Germany) at a flow rate of 250 nL/min at 50 ◦C controlled by HyStar software (v6.0.30.0, Bruker Daltonik). The liquid chromatography (LC) run lasted for 80 min. A starting concentration of 2% buffer B increasing to 13% over the first 42 min

 doi:10.20944/preprints202312.0550.v1

was first performed and buffer B concentrations were increased up to 20% at 65 min; 30% at 70 min; 85% at 75 min and finally 85% for 5 min to wash the column. The temperature of the ion transfer capillary was set at 180 ° C. Ions were accumulated for 100 ms, and mobility separation was achieved by ramping the entrance potential from −160 V to −20 V within 114 ms. The acquisition of the MS and MS/MS mass spectra was done with average resolutions 50.000 FWHM full width at half maximum (mass range 100–1700 m/z), respectively. To enable the PASEF method, precursor m/z and mobility information was first derived from full scan TIMS-MS experiments (with a mass range of m/z 100–1700). The quadrupole isolation width was set to 2 and 3 Th and, for fragmentation, the collision energies varied between 31 and 52 eV depending on the precursor mass and charge. TIMS, MS operation and PASEF were controlled and synchronized using the control instrument software OtofControl 6.2.5 (Bruker Daltonik). LC-MS/MS data were acquired using the PASEF method as previously described [60], with a total cycle time of 1.31 s, including 1 TIMS MS scan and 10 PASEF MS/MS scans. The 10 PASEF scans (100 ms each) contained, on average, 12 MS/MS scans per PASEF scan. Ion mobility-resolved mass spectra, nested ion mobility vs. m/z distributions, as well as summed fragment ion intensities were extracted from the raw data file with DataAnalysis 6.0 (Bruker Daltonik) (Adapt from [60]).

4.3.5. NanoLC-MS/MS Acquisition of Samples in diaPASEF Mode

Twenty samples were then analysed individually in diaPASEF mode. Each tryptic peptide sample, of approximately 400-500 ng each, was analysed under the conditions described above. These included the same analytical conditions (identical instrumentation, type of separation column and gradient length) and analysis on the same instrument (timsTOF Pro, Bruker Daltonik). For the development of the diaPASEF method, we used a method with an adapted instrument firmware to perform data-independent isolation of data from several 25 m/z wide precursor windows, also called segments, in a single TIMS separation (107.5 ms). We used a method with two boxes per segment in each 107.5 ms diaPASEF scan, *i.e.*, a total of thirty-two segments and sixty-four boxes, of which sixteen of these scans perfectly cover the diagonal area of doubly and triply charged peptides in the m/z and ion mobility output range. MS and MS/MS data were collected over the m/z range 100 - 1700 and over the mobility range from 1/K0 = 0.6 to 1/K0 = 1.6 Vs cm-2. During each data collection, each TIMS cycle was 1.25 seconds long and comprised 1 MS and 22 cycles of diaPASEF MS/MS segments, comprising 2, 3 or 4 boxes, to cover a total of 64 boxes defined in the acquisition method. The collision energy was increased linearly with mobility from 68 eV at 1/K0 = 1.6 Vs cm^{-2} to 25 eV at 1/K0=0.6 Vs cm^{-2}.

4.3.6. MS Data Processing

Ion mobility resolved mass spectra, nested ion mobility versus m/z distributions, and fragment ion intensity sums were extracted from the raw data file with DataAnalysis 6.0 (Bruker Daltonik). The signal-to-noise ratio (S/N) was increased by summing the individual TIMS scans. Mobility peak positions and half-peak widths were determined on the basis of extracted ion mobilograms (EIM, ± 0.05 Da) using the peak detection algorithm implemented in the DataAnalysis software. Feature detection was also performed using DataAnalysis 6.0 software; stored at the raw data level (.d).

4.3.7. Data Analysis–Library Generation

For the resource library, the DDA raw files were analyzed in Spectronaut software version 16 (Biognosys, Schlieren, Switzerland), using the integrated Pulsar search engine and a search schema with default settings to generate respective spectral library.

The calibration search was dynamic and MS1, MS2 correction factor was 1. Data were searched against the UniProt KB Human database (20,594 sequences, downloaded on February, 2023), with trypsin/P as the protease with up to two missed cleavages. To account for post-translational modifications and chemical labelling settings, carbamidomethylation of cysteine residues was defined as a fixed modification, and methionine oxidation and acetylation of protein N-termini were

 doi:10.20944/preprints202312.0550.v1

defined as variable modifications. A FDR less than 1% was ensured on precursor, peptide and protein level.

4.3.8. Library Search of DIA Data

Prior library-based analysis of the DIA data, the raw files were converted into htrms files using the htrms converter (Biognosys). MS1 and MS2 data were centroided during conversion. The other parameters were set to default. The htrms files were then analyzed with Spectronaut using the previously generated libraries and default settings. The results were filtered by a 1% FDR on precursor, peptide and protein level using a target-decoy approach, which corresponds to a q-value ≤ 0.01 [61].

4.3.9. Quantification and Statistical Analyses of Proteomics Data

Quantification based on average top 3 and data normalization were performed using Spectronaut software. Given the number of samples analysed (less than 500 individuals), the local regression normalization described by Callister et al. [62] was carried out for the whole dataset. A t-test was applied and data were filtered by a Qvalue (multiple testing corrected p-value) of 0.05 and an absolute log2 ratio of 0.58, which correspond to a fold change of 1.5.

The resulting differential proteins were classified using unsupervised Bayesian clustering [63], according to their expression in the two groups (H-NAIVE, H-FCH). Each generated cluster was pooled according to protein expression, and then used for Gene Ontology (GO) term enrichment analysis. The Cytoscape plug-in Bingo [64] was used with the following parameters: right-sided hypergeometric test with a Benjamini-Hochberg correction, a p-value threshold of 0.05, and the use of all quantified proteins as the reference set. Visualization of enriched gene ontology terms was conducted following the protocol described by [65]. Principal component analysis (PCA) and volcano were generated by Spectronaut. Box plots were performed using the MetaboAnalyst 5.0 web server [66].

5. Conclusions

We have recently demonstrated the beneficial effects of FCH for nutricosmetic applications. In this study, through an ex vivo clinical approach coupled with in vitro HDF experiments and proteomic analysis by diaPASEF, we highlighted the beneficial effects of FCH in healing process and its potential underlying mechanisms. Our results demonstrate that human FCH-enriched serum improved wound closure in an in vitro scratch assay. In support, proteins with anti-inflammatory and immunomodulatory properties and proteins prone to promote hydration and ECM stability showed increased expression after exposure to FCH-enriched serum. Altogether, these data provide valuable new insights on the mechanisms likely contributing to the beneficial impact of FCH on human skin functionality by supporting WH and skin regeneration. Further studies are required to reinforce these preliminary data and investigate the role of FCH in skin diseases, such as DA and psoriasis, which are tightly associated with alterations in the immune system.

6. Patents

The human ex vivo methodology used in this study has been registered as a written invention disclosure by the French National Institute for Agronomic, Food and Environment Research (INRAE) (DIRV#18-0058). Clinic'n'Cell® has been registered as a mark.

Supplementary Materials: The following supporting information can be downloaded at the website of this paper posted on Preprints.org, Table S1: List of quantified proteins after Spectronaut processing and data analyses, two groups H-FCH/H-NAIVE (n = 10/group); Table S2: List of differential proteins filtered by Qvalue (0.05) and absolute log2 ratio (0.58) in 1st tab and filtered only by Qvalue (0.05) in 2nd tab; Table S3: Enriched GO terms and associated proteins from cluster C1-C2; Matched GO terms and associated proteins from cluster C3-C6. Figure S1: Peptide molecular weight (MW) repartition of fish cartilage hydrolysate, obtained by gel permeation HPLC-UV (given as indicative value).

Author Contributions: Conceptualization, J.L.F., Y.W. and C.P.; formal analysis, R.L. and F.W.; investigation, J.L.F., A.G., R.L. and F.W.; methodology, A.G., R.L., F.W., L.B.W., E.C., Y.W. and C.P.; project administration, L.B.W., E.B. and E.C.; writing, J.L.F. and Y.W.; writing–review & editing, J.L.F., A.G., E.B., E.C., Y.W., and C.P. All authors have read and agreed to the published version of the manuscript.

Funding: This research was funded by Abyss Ingredients. This work was also supported by structural grants from Biogenouest, Infrastructures en Biologie Santé et Agronomie (IBiSA), and the Conseil Régional de Bretagne awarded to C.P. The contribution of Y.W. was supported by INRAE.

Institutional Review Board Statement: The study was conducted in accordance with the Declaration of Helsinki, and approved by the French Ethical Committee (2021-ND77 RIPH2 HPS/N◦ SI RIPH: 21.01436.000014/N◦ EudraCT/ID RCB: 2021-A01773-38/Comité de Protection des Personnes CPP Paris, Ile-de-France 1; approved 08 October 2021).

Informed Consent Statement: Informed consent was obtained from all subjects involved in the study.

Data Availability Statement: The mass spectrometry proteomics data have been deposited to the ProteomeXchange Consortium via the PRIDE [67] partner repository with the dataset identifier PXD046125. Reviewer account details: Username: reviewer_pxd046125@ebi.ac.uk; Password: qvNqfP9a. For the raw data, T0 corresponds to H-NAIVE while TP corresponds to H-FCH.

Conflicts of Interest: A.G., R.L., E.C. and C.P. have no conflict of interest to declare. F.W. and L.B.-W. work for Clinic'n'Cell SAS. Y.W. provides scientific consulting for Clinic'n'Cell SAS. J.L.F. and E.B. work for Abyss Ingredients and provided the ingredients. Financial support was provided as service provision to Clinic'n'Cell SAS for the conduct of *the ex vivo* experimentations and to Protim for the conduct of the diaPASEF proteomic analyses. The funder had no role in the experimental design of the study or in the data collection. From Abyss Ingredients, J.L.F. contributed to the data interpretation and to the writing of the manuscript, while E.B. supervised this work and reviewed the manuscript. The funder decided with the authors to publish the results.

References

1. Elias, P.M. The Skin Barrier as an Innate Immune Element. *Semin Immunopathol* **2007**, *29*, 3–14, doi:10.1007/s00281-007-0060-9.
2. Shpichka, A.; Butnaru, D.; Bezrukov, E.A.; Sukhanov, R.B.; Atala, A.; Burdukovskii, V.; Zhang, Y.; Timashev, P. Skin Tissue Regeneration for Burn Injury. *Stem Cell Res Ther* **2019**, *10*, 94, doi:10.1186/s13287-019-1203-3.
3. Quondamatteo, F. Skin and Diabetes Mellitus: What Do We Know? *Cell Tissue Res* **2014**, *355*, 1–21, doi:10.1007/s00441-013-1751-2.
4. Boguniewicz, M.; Leung, D.Y.M. Atopic Dermatitis: A Disease of Altered Skin Barrier and Immune Dysregulation. *Immunological Reviews* **2011**, *242*, 233–246, doi:10.1111/j.1600-065X.2011.01027.x.
5. Paller, A.S.; Kong, H.H.; Seed, P.; Naik, S.; Scharschmidt, T.C.; Gallo, R.L.; Luger, T.; Irvine, A.D. The Microbiome in Patients with Atopic Dermatitis. *Journal of Allergy and Clinical Immunology* **2019**, *143*, 26–35, doi:10.1016/j.jaci.2018.11.015.
6. Elder, J.T.; Bruce, A.T.; Gudjonsson, J.E.; Johnston, A.; Stuart, P.E.; Tejasvi, T.; Voorhees, J.J.; Abecasis, G.R.; Nair, R.P. Molecular Dissection of Psoriasis: Integrating Genetics and Biology. *Journal of Investigative Dermatology* **2010**, *130*, 1213–1226, doi:10.1038/jid.2009.319.
7. Sorg, H.; Tilkorn, D.J.; Hager, S.; Hauser, J.; Mirastschijski, U. Skin Wound Healing: An Update on the Current Knowledge and Concepts. *European Surgical Research* **2016**, *58*, 81–94, doi:10.1159/000454919.
8. Geahchan, S.; Baharlouei, P.; Rahman, A. Marine Collagen: A Promising Biomaterial for Wound Healing, Skin Anti-Aging, and Bone Regeneration. *Marine Drugs* **2022**, *20*, 61, doi:10.3390/md20010061.
9. León-López, A.; Morales-Peñaloza, A.; Martínez-Juárez, V.M.; Vargas-Torres, A.; Zeugolis, D.I.; Aguirre-Álvarez, G. Hydrolyzed Collagen—Sources and Applications. *Molecules* **2019**, *24*, 4031, doi:10.3390/molecules24224031.
10. Hu, Z.; Yang, P.; Zhou, C.; Li, S.; Hong, P. Marine Collagen Peptides from the Skin of Nile Tilapia (Oreochromis Niloticus): Characterization and Wound Healing Evaluation. *Mar Drugs* **2017**, *15*, 102, doi:10.3390/md15040102.
11. Yang, T.; Zhang, K.; Li, B.; Hou, H. Effects of Oral Administration of Peptides with Low Molecular Weight from Alaska Pollock (Theragra Chalcogramma) on Cutaneous Wound Healing. *Journal of Functional Foods* **2018**, *48*, 682–691, doi:10.1016/j.jff.2018.08.006.
12. Wang, J.; Xu, M.; Liang, R.; Zhao, M.; Zhang, Z.; Li, Y. Oral Administration of Marine Collagen Peptides Prepared from Chum Salmon (Oncorhynchus Keta) Improves Wound Healing Following Cesarean Section in Rats. *Food & Nutrition Research* **2015**, *59*, 26411, doi:10.3402/fnr.v59.26411.

13. Zhang, Z.; Wang, J.; Ding, Y.; Dai, X.; Li, Y. Oral Administration of Marine Collagen Peptides from Chum Salmon Skin Enhances Cutaneous Wound Healing and Angiogenesis in Rats. *Journal of the Science of Food and Agriculture* **2011**, *91*, 2173–2179, doi:10.1002/jsfa.4435.
14. Valcarcel, J.; Novoa-Carballal, R.; Pérez-Martín, R.I.; Reis, R.L.; Vázquez, J.A. Glycosaminoglycans from Marine Sources as Therapeutic Agents. *Biotechnology Advances* **2017**, *35*, 711–725, doi:10.1016/j.biotechadv.2017.07.008.
15. Campo, G.M.; Avenoso, A.; Campo, S.; D'Ascola, A.; Traina, P.; Samà, D.; Calatroni, A. Glycosaminoglycans Modulate Inflammation and Apoptosis in LPS-Treated Chondrocytes. *Journal of Cellular Biochemistry* **2009**, *106*, 83–92, doi:10.1002/jcb.21981.
16. Tan, G.-K.; Tabata, Y. Chondroitin-6-Sulfate Attenuates Inflammatory Responses in Murine Macrophages via Suppression of NF-κB Nuclear Translocation. *Acta Biomaterialia* **2014**, *10*, 2684–2692, doi:10.1016/j.actbio.2014.02.025.
17. Henrotin, Y.; Herman, J.; Uebelhoer, M.; Wauquier, F.; Boutin-Wittrant, L.; Donneau, A.-F.; Monseur, J.; Fotso, V.M.; Duquenne, M.; Wagner, M.; et al. Oral Supplementation with Fish Cartilage Hydrolysate in an Adult Population Suffering from Knee Pain and Function Discomfort: Results from an Innovative Approach Combining an Exploratory Clinical Study and an Ex Vivo Clinical Investigation. *BMC Musculoskeletal Disorders* **2023**, *24*, 748, doi:10.1186/s12891-023-06800-4.
18. Krichen, F.; Ghlissi, Z.; Abdallah, R.B.; Kallel, R.; Martinez-Alvarez, O.; Carmen Gómez-Guillén, M.; Sila, A.; Boudawara, T.; Sahnoun, Z.; Bougatef, A. Glycosaminoglycans from Grey Triggerfish and Smooth Hound Skins: Rheological, Anti-Inflammatory and Wound Healing Properties. *International Journal of Biological Macromolecules* **2018**, *118*, 965–975, doi:10.1016/j.ijbiomac.2018.06.132.
19. Wauquier, F.; Boutin-Wittrant, L.; Bouvret, E.; Le Faouder, J.; Roux, V.; Macian, N.; Pickering, G.; Wittrant, Y. Benefits of Circulating Human Metabolites from Fish Cartilage Hydrolysate on Primary Human Dermal Fibroblasts, an Ex Vivo Clinical Investigation for Skin Health Applications. *Nutrients* **2022**, *14*, 5027, doi:10.3390/nu14235027.
20. Maia Campos, P.M.B.G.; Franco, R.S.B.; Kakuda, L.; Cadioli, G.F.; Costa, G.M.D.; Bouvret, E. Oral Supplementation with Hydrolyzed Fish Cartilage Improves the Morphological and Structural Characteristics of the Skin: A Double-Blind, Placebo-Controlled Clinical Study. *Molecules* **2021**, *26*, 4880, doi:10.3390/molecules26164880.
21. Wauquier, F.; Daneault, A.; Granel, H.; Prawitt, J.; Fabien Soulé, V.; Berger, J.; Pereira, B.; Guicheux, J.; Rochefort, G.Y.; Meunier, N.; et al. Human Enriched Serum Following Hydrolysed Collagen Absorption Modulates Bone Cell Activity: From Bedside to Bench and Vice Versa. *Nutrients* **2019**, *11*, 1249, doi:10.3390/nu11061249.
22. Wauquier, F.; Mevel, E.; Krisa, S.; Richard, T.; Valls, J.; Hornedo-Ortega, R.; Granel, H.; Boutin-Wittrant, L.; Urban, N.; Berger, J.; et al. Chondroprotective Properties of Human-Enriched Serum Following Polyphenol Extract Absorption: Results from an Exploratory Clinical Trial. *Nutrients* **2019**, *11*, 3071, doi:10.3390/nu11123071.
23. Kleinnijenhuis, A.J.; van Holthoon, F.L.; Maathuis, A.J.H.; Vanhoecke, B.; Prawitt, J.; Wauquier, F.; Wittrant, Y. Non-Targeted and Targeted Analysis of Collagen Hydrolysates during the Course of Digestion and Absorption. *Anal Bioanal Chem* **2020**, *412*, 973–982, doi:10.1007/s00216-019-02323-x.
24. Wauquier, F.; Boutin-Wittrant, L.; Viret, A.; Guilhaudis, L.; Oulyadi, H.; Bourafai-Aziez, A.; Charpentier, G.; Rousselot, G.; Cassin, E.; Descamps, S.; et al. Metabolic and Anti-Inflammatory Protective Properties of Human Enriched Serum Following Artichoke Leaf Extract Absorption: Results from an Innovative Ex Vivo Clinical Trial. *Nutrients* **2021**, *13*, 2653, doi:10.3390/nu13082653.
25. Wauquier, F.; Boutin-Wittrant, L.; Pourtau, L.; Gaudout, D.; Moras, B.; Vignault, A.; Monchaux De Oliveira, C.; Gabaston, J.; Vaysse, C.; Bertrand, K.; et al. Circulating Human Serum Metabolites Derived from the Intake of a Saffron Extract (Safr'InsideTM) Protect Neurons from Oxidative Stress: Consideration for Depressive Disorders. *Nutrients* **2022**, *14*, 1511, doi:10.3390/nu14071511.
26. Demichev, V.; Szyrwiel, L.; Yu, F.; Teo, G.C.; Rosenberger, G.; Niewienda, A.; Ludwig, D.; Decker, J.; Kaspar-Schoenefeld, S.; Lilley, K.S.; et al. Dia-PASEF Data Analysis Using FragPipe and DIA-NN for Deep Proteomics of Low Sample Amounts. *Nat Commun* **2022**, *13*, 3944, doi:10.1038/s41467-022-31492-0.
27. Guergues, J.; Wohlfahrt, J.; Stevens, S.M.Jr. Enhancement of Proteome Coverage by Ion Mobility Fractionation Coupled to PASEF on a TIMS–QTOF Instrument. *J. Proteome Res.* **2022**, *21*, 2036–2044, doi:10.1021/acs.jproteome.2c00336.
28. Sodhi, H.; Panitch, A. Glycosaminoglycans in Tissue Engineering: A Review. *Biomolecules* **2021**, *11*, 29, doi:10.3390/biom11010029.
29. Cheng, F.; Shen, Y.; Mohanasundaram, P.; Lindström, M.; Ivaska, J.; Ny, T.; Eriksson, J.E. Vimentin Coordinates Fibroblast Proliferation and Keratinocyte Differentiation in Wound Healing via TGF-β–Slug Signaling. *Proceedings of the National Academy of Sciences* **2016**, *113*, E4320–E4327, doi:10.1073/pnas.1519197113.

30. Liarte, S.; Bernabé-García, Á.; Nicolás, F.J. Role of TGF-β in Skin Chronic Wounds: A Keratinocyte Perspective. *Cells* **2020**, *9*, 306, doi:10.3390/cells9020306.
31. Law, R.H.; Zhang, Q.; McGowan, S.; Buckle, A.M.; Silverman, G.A.; Wong, W.; Rosado, C.J.; Langendorf, C.G.; Pike, R.N.; Bird, P.I.; et al. An Overview of the Serpin Superfamily. *Genome Biology* **2006**, *7*, 216, doi:10.1186/gb-2006-7-5-216.
32. Park, D.J.; Duggan, E.; Ho, K.; Dorschner, R.A.; Dobke, M.; Nolan, J.P.; Eliceiri, B.P. Serpin-Loaded Extracellular Vesicles Promote Tissue Repair in a Mouse Model of Impaired Wound Healing. *Journal of Nanobiotechnology* **2022**, *20*, 474, doi:10.1186/s12951-022-01656-7.
33. Grimstein, C.; Choi, Y.-K.; Satoh, M.; Lu, Y.; Wang, X.; Campbell-Thompson, M.; Song, S. Combination of Alpha-1 Antitrypsin and Doxycycline Suppresses Collagen-Induced Arthritis. *The Journal of Gene Medicine* **2010**, *12*, 35–44, doi:10.1002/jgm.1409.
34. Janciauskiene, S.M.; Nita, I.M.; Stevens, T. A1-Antitrypsin, Old Dog, New Tricks: A1-Antitrypsin Exerts in Vitro Anti-Inflammatory Activity in Human Monocytes by Elevating cAMP. *Journal of Biological Chemistry* **2007**, *282*, 8573–8582, doi:10.1074/jbc.M607976200.
35. Congote, L.F.; Temmel, N.; Sadvakassova, G.; Dobocan, M.C. Comparison of the Effects of Serpin A1, a Recombinant Serpin A1-IGF Chimera and Serpin A1 C-Terminal Peptide on Wound Healing. *Peptides* **2008**, *29*, 39–46, doi:10.1016/j.peptides.2007.10.011.
36. Hoffmann, D.C.; Textoris, C.; Oehme, F.; Klaassen, T.; Goppelt, A.; Römer, A.; Fugmann, B.; Davidson, J.M.; Werner, S.; Krieg, T.; et al. Pivotal Role for A1-Antichymotrypsin in Skin Repair*. *Journal of Biological Chemistry* **2011**, *286*, 28889–28901, doi:10.1074/jbc.M111.249979.
37. Kirschfink, M.; Nürnberger, W. C1 Inhibitor in Anti-Inflammatory Therapy: From Animal Experiment to Clinical Application. *Molecular Immunology* **1999**, *36*, 225–232, doi:10.1016/S0161-5890(99)00048-6.
38. Begieneman, M.P.V.; Kubat, B.; Ulrich, M.M.W.; Hahn, N.E.; Stumpf-Stolker, Y.; Tempelaars, M.; Middelkoop, E.; Zeerleder, S.; Wouters, D.; van Ham, M.S.; et al. Prolonged C1 Inhibitor Administration Improves Local Healing of Burn Wounds and Reduces Myocardial Inflammation in a Rat Burn Wound Model. *Journal of Burn Care & Research* **2012**, *33*, 544–551, doi:10.1097/BCR.0b013e31823bc2fc.
39. Schraufstatter, I.U.; Khaldoyanidi, S.K.; DiScipio, R.G. Complement Activation in the Context of Stem Cells and Tissue Repair. *World J Stem Cells* **2015**, *7*, 1090–1108, doi:10.4252/wjsc.v7.i8.1090.
40. Sinno, H.; Malholtra, M.; Lutfy, J.; Jardin, B.; Winocour, S.; Brimo, F.; Beckman, L.; Watters, K.; Philip, A.; Williams, B.; et al. Topical Application of Complement C3 in Collagen Formulation Increases Early Wound Healing. *Journal of Dermatological Treatment* **2013**, *24*, 141–147, doi:10.3109/09546634.2011.631977.
41. Sinno, H.; Malhotra, M.; Lutfy, J.; Jardin, B.; Winocour, S.; Brimo, F.; Beckman, L.; Watters, K.; Philip, A.; Williams, B.; et al. Accelerated Wound Healing with Topical Application of Complement C5. *Plastic and Reconstructive Surgery* **2012**, *130*, 523, doi:10.1097/PRS.0b013e31825dc02d.
42. Man, R.C.; Idrus, R.B.H.; Ibrahim, W.I.W.; Saim, A.B.; Lokanathan, Y. Secretome Analysis of Human Nasal Fibroblast Identifies Proteins That Promote Wound Healing. In; Advances in Experimental Medicine and Biology; Springer International Publishing: Cham; pp. 1–18.
43. Hochepied, T.; Berger, F.G.; Baumann, H.; Libert, C. A1-Acid Glycoprotein: An Acute Phase Protein with Inflammatory and Immunomodulating Properties. *Cytokine & Growth Factor Reviews* **2003**, *14*, 25–34, doi:10.1016/S1359-6101(02)00054-0.
44. Vandooren, J.; Itoh, Y. Alpha-2-Macroglobulin in Inflammation, Immunity and Infections. *Frontiers in Immunology* **2021**, *12*.
45. Nishio, N.; Ito, S.; Suzuki, H.; Isobe, K.-I. Antibodies to Wounded Tissue Enhance Cutaneous Wound Healing. *Immunology* **2009**, *128*, 369–380, doi:10.1111/j.1365-2567.2009.03119.x.
46. Noh, J.Y.; Shin, J.U.; Kim, J.H.; Kim, S.H.; Kim, B.-M.; Kim, Y.H.; Park, S.; Kim, T.-G.; Shin, K.-O.; Park, K.; et al. ZAG Regulates the Skin Barrier and Immunity in Atopic Dermatitis. *Journal of Investigative Dermatology* **2019**, *139*, 1648-1657.e7, doi:10.1016/j.jid.2019.01.023.
47. Haque, M.; Siegel, R.J.; Fox, D.A.; Ahmed, S. Interferon-Stimulated GTPases in Autoimmune and Inflammatory Diseases: Promising Role for the Guanylate-Binding Protein (GBP) Family. *Rheumatology* **2021**, *60*, 494–506, doi:10.1093/rheumatology/keaa609.
48. Bowcock, A.M.; Shannon, W.; Du, F.; Duncan, J.; Cao, K.; Aftergut, K.; Catier, J.; Fernandez-Vina, M.A.; Menter, A. Insights into Psoriasis and Other Inflammatory Diseases from Large-Scale Gene Expression Studies. *Human Molecular Genetics* **2001**, *10*, 1793–1805, doi:10.1093/hmg/10.17.1793.
49. Park, S.Y.; Gupta, D.; Hurwich, R.; Kim, C.H.; Dziarski, R. Peptidoglycan Recognition Protein Pglyrp2 Protects Mice from Psoriasis-Like Skin Inflammation by Promoting Treg and Limiting Th17 Responses. *J Immunol* **2011**, *187*, 5813–5823, doi:10.4049/jimmunol.1101068.
50. Chen, C.-C.; Mo, F.-E.; Lau, L.F. The Angiogenic Factor Cyr61 Activates a Genetic Program for Wound Healing in Human Skin Fibroblasts *. *Journal of Biological Chemistry* **2001**, *276*, 47329–47337, doi:10.1074/jbc.M107666200.
51. Bost, F.; Diarra-Mehrpour, M.; Martin, J.-P. Inter-α-Trypsin Inhibitor Proteoglycan Family. *European Journal of Biochemistry* **1998**, *252*, 339–346, doi:10.1046/j.1432-1327.1998.2520339.x.

52. Yamashita, T.; Asano, Y.; Saigusa, R.; Taniguchi, T.; Nakamura, K.; Miura, S.; Toyama, T.; Takahashi, T.; Ichimura, Y.; Hirabayashi, M.; et al. Increased Expression of Aquaporin-1 in Dermal Fibroblasts and Dermal Microvascular Endothelial Cells Possibly Contributes to Skin Fibrosis and Edema in Patients with Systemic Sclerosis. *Journal of Dermatological Science* **2019**, *93*, 24–32, doi:10.1016/j.jdermsci.2018.09.007.
53. Chmilewsky, F.; Jeanneau, C.; Laurent, P.; About, I. Pulp Fibroblasts Synthesize Functional Complement Proteins Involved in Initiating Dentin-Pulp Regeneration. *Am J Pathol* **2014**, *184*, 1991–2000, doi:10.1016/j.ajpath.2014.04.003.
54. Kulics, J.; Circolo, A.; Strunk, R.C.; Colten, H.R. Regulation of Synthesis of Complement Protein C4 in Human Fibroblasts: Cell- and Gene-Specific Effects of Cytokines and Lipopolysaccharide. *Immunology* **1994**, *82*, 509–515.
55. Katz, Y.; Strunk, R.C. Synovial Fibroblast-like Cells Synthesize Seven Proteins of the Complement System. *Arthritis & Rheumatism* **1988**, *31*, 1365–1370, doi:10.1002/art.1780311104.
56. Loo, A.E.K.; Halliwell, B. Effects of Hydrogen Peroxide in a Keratinocyte-Fibroblast Co-Culture Model of Wound Healing. *Biochemical and Biophysical Research Communications* **2012**, *423*, 253–258, doi:10.1016/j.bbrc.2012.05.100.
57. Hong, Z.-X.; Zhu, S.-T.; Li, H.; Luo, J.-Z.; Yang, Y.; An, Y.; Wang, X.; Wang, K. Bioengineered Skin Organoids: From Development to Applications. *Military Med Res* **2023**, *10*, 40, doi:10.1186/s40779-023-00475-7.
58. Hijnen, D.; Knol, E.F.; Gent, Y.Y.; Giovannone, B.; Beijn, S.J.P.; Kupper, T.S.; Bruijnzeel-Koomen, C.A.F.M.; Clark, R.A. CD8+ T Cells in the Lesional Skin of Atopic Dermatitis and Psoriasis Patients Are an Important Source of IFN-γ, IL-13, IL-17, and IL-22. *Journal of Investigative Dermatology* **2013**, *133*, 973–979, doi:10.1038/jid.2012.456.
59. Yilmaz, O.; Com, E.; Lavigne, R.; Pineau, C.; Bobe, J. Liquid Chromatography and Tandem Mass Spectrometry in Label-Free Protein QuantificationProtein Quantification of Zebrafish (Danio Rerio)Zebrafish (Danio Rerio)Eggs. In *Germline Development in the Zebrafish: Methods and Protocols*; Dosch, R., Ed.; Methods in Molecular Biology; Springer US: New York, NY, 2021; pp. 277–290 ISBN 978-1-07-160970-5.
60. Banliat, C.; Tsikis, G.; Labas, V.; Teixeira-Gomes, A.-P.; Com, E.; Lavigne, R.; Pineau, C.; Guyonnet, B.; Mermillod, P.; Saint-Dizier, M. Identification of 56 Proteins Involved in Embryo–Maternal Interactions in the Bovine Oviduct. *Int J Mol Sci* **2020**, *21*, 466, doi:10.3390/ijms21020466.
61. Bruderer, R.; Bernhardt, O.M.; Gandhi, T.; Xuan, Y.; Sondermann, J.; Schmidt, M.; Gomez-Varela, D.; Reiter, L. Optimization of Experimental Parameters in Data-Independent Mass Spectrometry Significantly Increases Depth and Reproducibility of Results *. *Molecular & Cellular Proteomics* **2017**, *16*, 2296–2309, doi:10.1074/mcp.RA117.000314.
62. Callister, S.J.; Barry, R.C.; Adkins, J.N.; Johnson, E.T.; Qian, W.-J.; Webb-Robertson, B.-J.M.; Smith, R.D.; Lipton, M.S. Normalization Approaches for Removing Systematic Biases Associated with Mass Spectrometry and Label-Free Proteomics. *J Proteome Res* **2006**, *5*, 277–286, doi:10.1021/pr050300l.
63. Achcar, F.; Camadro, J.-M.; Mestivier, D. AutoClass@IJM: A Powerful Tool for Bayesian Classification of Heterogeneous Data in Biology. *Nucleic Acids Res* **2009**, *37*, W63–W67, doi:10.1093/nar/gkp430.
64. Maere, S.; Heymans, K.; Kuiper, M. BiNGO: A Cytoscape Plugin to Assess Overrepresentation of Gene Ontology Categories in Biological Networks. *Bioinformatics* **2005**, *21*, 3448–3449, doi:10.1093/bioinformatics/bti551.
65. Bonnot, T.; Gillard, M.; Nagel, D. A Simple Protocol for Informative Visualization of Enriched Gene Ontology Terms. *BIO-PROTOCOL* **2019**, *9*, doi:10.21769/BioProtoc.3429.
66. Xia, J.; Psychogios, N.; Young, N.; Wishart, D.S. MetaboAnalyst: A Web Server for Metabolomic Data Analysis and Interpretation. *Nucleic Acids Research* **2009**, *37*, W652–W660, doi:10.1093/nar/gkp356.
67. Perez-Riverol, Y.; Bai, J.; Bandla, C.; García-Seisdedos, D.; Hewapathirana, S.; Kamatchinathan, S.; Kundu, D.J.; Prakash, A.; Frericks-Zipper, A.; Eisenacher, M.; et al. The PRIDE Database Resources in 2022: A Hub for Mass Spectrometry-Based Proteomics Evidences. *Nucleic Acids Research* **2022**, *50*, D543–D552, doi:10.1093/nar/gkab1038.